Reductive Elimination of d^8-Organotransition Metal Complexes

Kazuyuki TATSUMI, Roald HOFFMANN,* Akio YAMAMOTO,** and John K. STILLE***

Department of Chemistry, Cornell University, Ithaca, New York 14853, U.S.A.

** *Research Laboratory of Resources Utilization, Tokyo Institute of Technology, Nagatsuta, Midori-ku, Yokohama 227*

*** *Department of Chemistry, Colorado State University, Fort Collins, Colorado 80523, U.S.A.*

(Received August 30, 1980)

A theoretical analysis of two aspects of the mechanism of reductive elimination is presented—how the choice of central metal and peripheral ligands affects the activation energy for reductive elimination from a four-coordinate $MR_2(PR_3)_2$ complex and how ligand asymmetry controls *cis-trans* rearrangements and elimination pathways proceeding through three-coordinate intermediates. The following conclusions emerge: (1) In the four-coordinate complex, the better the σ-donating capability of the leaving groups, the more facile the elimination; (2) Stronger donor ligands *trans* to the leaving groups will increase the barrier to elimination; (3) The reductive elimination barrier in four-coordinate complexes is controlled by the energy of an antisymmetric b_2 orbital, which in turn depends on the energy of the metal levels. The activation energy for such direct reductive elimination should be, and is, substantially lower for Ni than for Pt or Pd; (4) T-shaped *trans* $PdLR_2$, arising from dissociation of L in PdL_2R_2, will encounter a substantial barrier to polytopal rearrangement to *cis* $PdLR_2$, which in turn has an open channel for reductive elimination of R_2; (5) If the leaving groups are poor donors, *cis-trans* isomerization in the three-coordinate manifold should be easier than elimination.

The coupling of two alkyl moieties into an alkane, *e.g.* (1), is a reaction efficiently accomplished by a number of d^8 transition metal centers—Ni(II), Pd(II),

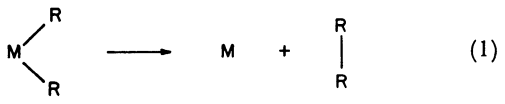

(1)

Pt(II), Au(III). But the simple form of the summary equation (1) for this process masks a multitude of mechanistic choices. Let us examine some of the possibilities in Scheme 1.

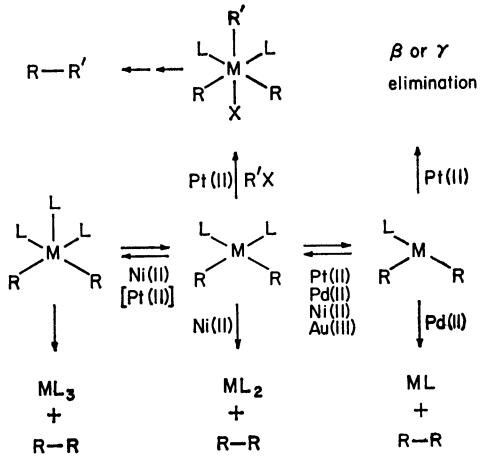

Scheme 1.

The most common starting point for these reactions is a preformed square-planar 16 electron, d^8 dialkyl (or tri-or tetraalkyl for Au(III)) complex which appears in the middle of the Scheme. The two other ligands, marked L, are typically phosphines. Depending on the size and electronic characteristics of the phosphine substituents one may observe associative or dissociative steps away from the four-coordinate complex. Both elementary processes have been clearly demonstrated in the Grubbs system, where M=Ni(II) and R_2 is a tetramethylene bridge.[1,2] Evidence is in fact in hand for the dissociative step in most such reactions.

The four-coordinate complex eliminates R–R cleanly and easily in the Ni(II) case only. For Pd(II) the work of the Yamamoto[3] and Stille[4] groups and for Au(III) of the Kochi group[5] has produced kinetic evidence for elimination from a three-coordinate intermediate. Pt(II) apparently does not eliminate R–R readily.[6] The Whitesides group[6a] has demonstrated β or γ elimination (where feasible) through a three-coordinate intermediate, while Puddephatt and coworkers[7] have found elimination reactions, but only after oxidative addition of an RX.

No stereochemical implications were meant to be drawn from Scheme 1. In fact the mechanistic possibilities are enriched by the range of equilibrium geometries and polytopal rearrangements available to the various intermediates. Some of the geometrical extremes are drawn in **1**—**9**. For the square-planar

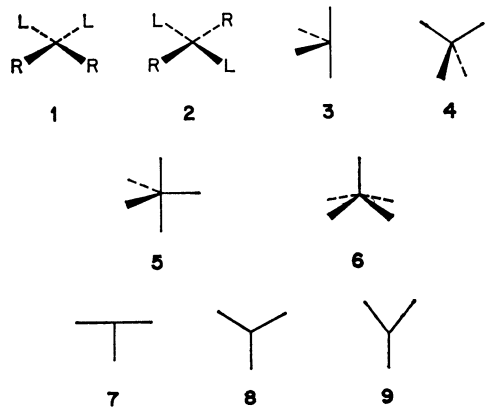

geometry one has available the *cis* and *trans* isomers **1** and **2**, and indeed the mechanism of elimination from either starting point has been studied. Some recent theoretical work[8] on the Grubbs system has focussed on another possible low-spin intermediate—the C_{2v} *cis*-octahedral fragment **3**. And at least for Ni(II) one has to worry about the tetrahedral, presumably high-spin,

alternative **4**. Even more geometrical isomers are available for a five-coordinate structure—here we remind ourselves only of the underlying geometries, the trigonal bipyramid **5** and the aquare pyramid **6**. For the three-coordinate geometry the idealized trigonal D_{3h} geometry **8** might seem to be the geometry of choice. But for reasons that are well understood,[5b] this most symmetrical structure is unlikely, and instead we must examine "T" and "Y"-shaped C_{2v} deformations, **7** and **9**. Mind you, these are only idealized geometrical extremes—the real molecules will certainly depart, to a variable degree, from these structures.

Our goal is a comprehensive theoretical understanding of this reaction type. Theoretical analyses of reductive elimination exist—the early and important work of Pearson[9] and of Braterman and Cross,[10] the more comprehensive and detailed approach of Åkermark and coworkers[11]—to mention some of the studies of this reaction. We ourselves have contributed an analysis of competitive elimination from three- and four-coordinate alternatives in the Au(III) system,[5b] and in work to be published still have investigated the nickellacyclopentane fragmenations.[8] All of these studies, those of others and ours as well, encounter one fundamental problem: *The reductive elimination is symmetry-allowed for many (not all) polytopal geometries of the three-, four-, and five-coordinate structures of Scheme 1. Why then does one metal choose one route, while a second metal opts for another?* We will try to give a partial answer to this question in this paper. We will also show how the electronic asymmetry of the ligand set controls the detailed mode of alkane elimination.

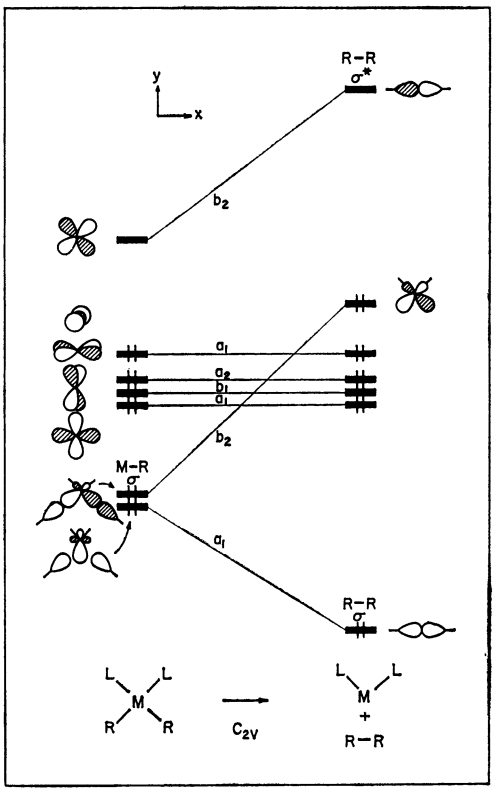

Fig. 1. Schematic correlation diagram for the elimination of R–R from a square-planar d^8 transition metal complex ML_2R_2. The reaction pathway maintains C_{2v} symmetry.

Reductive Elimination from *cis* Four-coordinate Complexes

The basic reaction, *cis* d^8 L_2MR_2 to d^{10} L_2M and R_2, is symmetry-allowed for a least motion C_{2v} departure.[8-11] A schematic correlation diagram to a bent ML_2 (the adjustment in making ML_2 linear is minor) is shown in Fig. 1. As usual these correlation diagrams abstract reality by proceeding from a semi-localized starting point in which only orbitals essential to the reaction are included.[12] Thus in the present case the orbitals in the diagram for L_2MR_2 are the five d-block orbitals of the metal and the two σ orbitals of the MR_2 unit. For ML_2+R_2 we have the R_2 σ and σ^* levels and the five metal d orbitals. The reality must be that these orbitals are not so simple and substantial mixing between the orbitals illustrated, as well as with others, not included in the figure, must occur. The purpose of these diagrams is to decide whether a level crossing does or does not occur—the actual details of the levels we will learn from a full calculation.

There is nevertheless one general feature of this allowed reaction that is evident from the figure and that we will return to later. This is the required evolution of one MR_2 bonding orbital, b_2 in symmetry,[13] into a primarily metal d orbital of the same symmetry, *i.e.* *xy* in a linear ML_2. This is indicated in **10**→**11**. Note

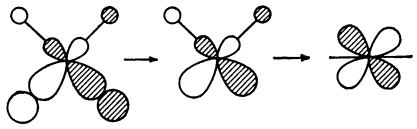

10 **11**

the loss of M–R bonding and electron transfer to the metal implied by this correlation. These will be important.

Our detailed analysis of the elimination reaction was carried out by means of extended Hückel calculations, with parameters specified in Appendix I. In several cases three degrees of freedom were studied, as illustrated in **12**: the angle between the leaving groups, φ; the separa-

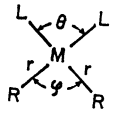

12

tion from the metal to these leaving R's, r; and the angle between the remaining. ligands, θ. As in our previous study of the Au(III) system[5b] we found that the essential features of the elimination were revealed in angular variations alone, *i.e.* changes of θ and φ at constant M–R separation. This is just as well, for the extended Hückel method is not good at representing correctly degrees of freedom in which distances are varied.

The ligands of course play a vital role in determining the feasibility of any reductive elimination. We carried out calculations with PH_3 and CH_3 ligands. These

led us to focus on the σ donor or acceptor strength of the ligands. Our interpretation was easiest made on a still simpler "hydride model." Here the ligands were simply hydrogen 1s functions with modified valence state ionization potentials. We called the two extremes A and D. A and D are hydrogen atoms, the 1s orbital energies of which are set to be -14.34 and -11.75 eV, respectively. The value -14.34 eV is the calculated orbital energy of a lone pair in PH_3 and -11.75 eV corresponds to that of a lone pair in CH_3^-. Thus A^- may be a model for PH_3 and D^- for CH_3^-. Or one can regard A as a poor donor ligand and D as a strong donor ligand.

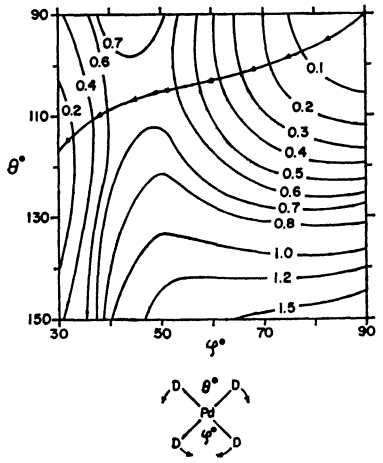

Fig. 2. Potential energy surface for variation of the two D–Pd–D angles, θ and φ, in planar PdD_4^{2-}. The energy contours are in electron volts relative to the square-planar geometry ($\theta=\varphi=90°$). A line with arrows indicates a reaction path corresponding to the elimination of D_2 from PdD_4^{2-}.

A potential energy surface in θ and φ for the elimination of D_2 from PdD_4^{2-} is illustrated in Fig. 2. The reaction path is shown by a line with arrows. In general the surface is quite analogous to that computed earlier by us for $Au(CH_3)_4^-$ [5b] —θ lags somewhat behind φ. Corresponding energy surfaces for the departure of A_2 and D_2 from PdA_2D_2 are illustrated in Fig. 3.

As these surfaces show, the reactions of these model compounds have a saddle point at around $\theta=100$—$110°$, $\varphi=40$—$50°$. When the two leaving ligands are gradually removed (r increased) at the point $\theta=110°$ $\varphi=30°$, no additional energy barrier was found. Thus each potential surface represents sufficiently well the reductive elimination reaction of a corresponding compound. The calculated activation energies for PdD_4^{2-}, $PdD_2A_2^{2-}$ (A leaving), and $PdA_2D_2^{2-}$ (D leaving) are 0.65, 2.7 (A_2 leaving), and 0.20 eV (D_2 leaving), respectively. We should not rely on these numbers in a quantitative sense, partly because we used the very simplified hypothetical hydride model (we will discuss this later), and partly because the calculational method is rather primitive. However the observed trends are quite suggestive. Here are two conclusions: (1) *The better the σ-donating capability of the leaving groups, the more readily the elimination reaction proceeds.* (2) *Stronger donor ligands which are* trans *to the leaving groups give a higher barrier for the elimination reaction.*

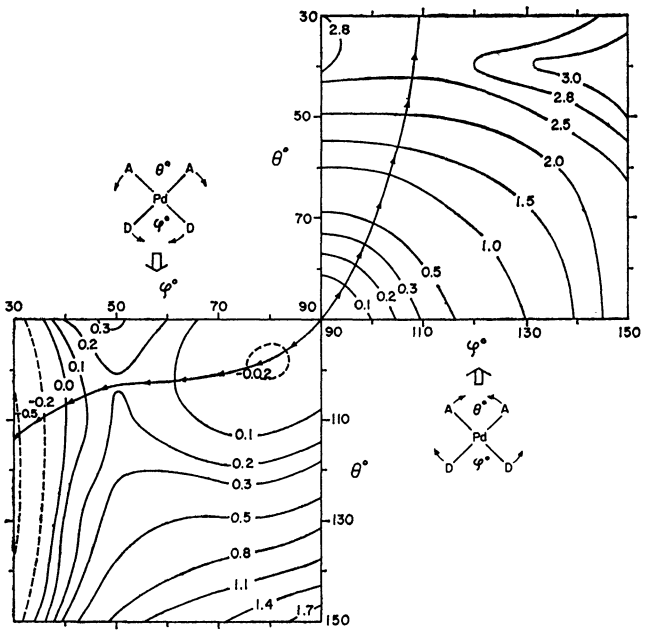

Fig. 3. Potential energy surface for variation of the two angles, θ (A–Pd–A) and φ (D–Pd–D), in planar Pd-$D_2A_2^{2-}$. The energy contours are in electron volts relative to the square-planar geometry ($\theta=\varphi=90°$). A line with arrows corresponds to reaction paths for D_2 elimination, lower left, and A_2 elimination, upper right.

The potential energy surface for $NiA_2D_2^{2-}$ is shown in Fig. 4, in which the leaving groups are the stronger donors D. Although this model compound is just the Ni analogue of $PdA_2D_2^{2-}$, the calculated potential surface of $NiA_2D_2^{2-}$ is quite different from that of $PdA_2D_2^{2-}$. While the elimination reaction of $PdA_2D_2^{2-}$ has a small but obvious energy barrier along the reaction coordinate, the reaction pathway of the Ni analogue is

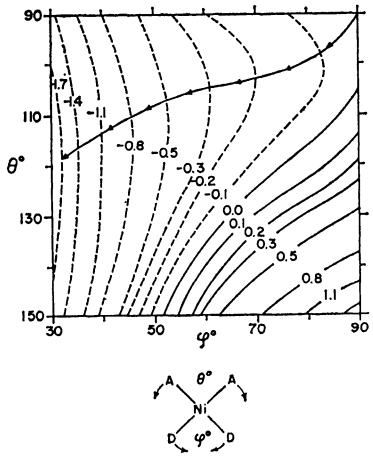

Fig. 4. Potential energy surface for variation of the two angles, θ(A–Ni–A) and φ(D–Ni–D), in planar $NiA_2D_2^{2-}$. The energy values on the contours are in electron volts relative to the square-planar geometry ($\theta=\varphi=90°$). A line with arrows indicates a reaction path for D_2 elimination from $NiA_2D_2^{2}$.

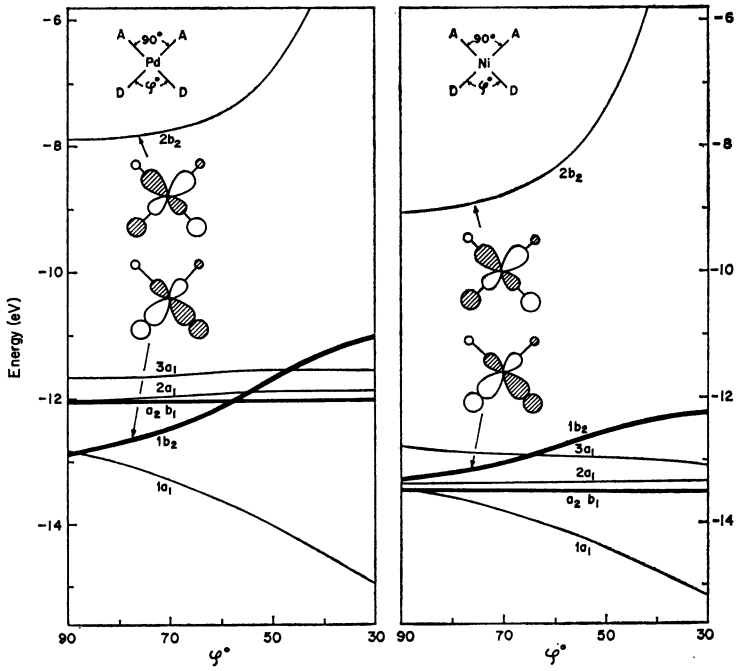

Fig. 5. Computed Walsh diagrams for $PdA_2D_2^{2-}$(left) and $NiA_2D_2^{2-}$(right), for decrease of the D–M–D angle φ. The A–M–A angle is kept at 90°. The $2b_2$ orbital is vacant.

merely downhill in energy and has no barrier.

Why is there such a different pattern for $PdA_2D_2^{2-}$ and $NiA_2D_2^{2-}$? The answer must lie, ultimately, in the Pd 4d *vs.* Ni 3d orbital energies. The effect is traced through Fig. 5, a set of Walsh diagrams. Each of the diagrams shows the variation of the important molecular orbital levels as a function of D–M–D (M=Pd or Ni) angle φ (90—30°), while A–M–A angle is kept at 90°. There are seven levels shown in Fig. 5. To make the correspondence to the schematic correlation diagram of Fig. 1 we can say that five of these seven levels are the d-block orbitals and two are M–D bonding orbitals. The reality is not so simple—there is extensive delocalization in some of the symmetry types. a_2 and b_1 are simple, pure metal yz and xz, unaffected by the elimination. $2a_1$ and $3a_1$ contain substantial d character, z^2 and x^2-y^2. But in fact they are part of a trio of a_1 orbitals which includes $1a_1$. We can think of these orbitals as derived from localized z^2, x^2-y^2 and the a_1 M–D σ bond combination. As the angle φ closes, one of the three a_1's goes down in energy and ends up as the σ bonding MO of D_2. Obviously the main stabilization which drives the elimination reaction is in these a_1 orbitals. However, the contribution to the total energy change of the three a_1 orbitals is quite similar in the Pd and Ni compounds. Thus the a_1 set does not differentiate between the two metals.

There are two b_2 orbitals in Fig. 5. We can think of them as bonding and antibonding M–D, A σ combinations, alternatively the higher orbital of the two could be thought of as that metal orbital, xy, which is destabilized by the square planar ligand field. Decreasing φ destabilizes both $1b_2$ and $2b_2$. The unoccupied $2b_2$ correlates to the eliminated D_2 σ^* level **13**, while the occupied $1b_2$ correlates to an MA_2 orbital which is nearly pure xy, **14**. The latter correlation was the one alluded to earlier, **10**→**11**.[14]

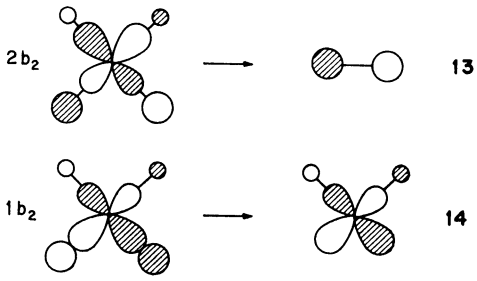

There is no level crossing for elimination of D_2 in either the Pd or the Ni case, confirming the simplified analysis of Fig. 1. The contrast between the potential energy surfaces for the two metals (Figs. 3 and 4) arises from the difference in slope of the $1b_2$ orbitals. As φ decreases $1b_2$ of $PdA_2D_2^{2-}$ is singificantly more pushed up than that of $NiA_2D_2^{2-}$, producing an energy barrier in the elimination of D_2 from the Pd compound.

The differential $1b_2$ destabilization may arise from two causes—decreasing M–D bonding and increasing D–D antibonding. Either way, it would be anticipated that if the D 1s orbital component in $1b_2$ is large, the destabilization of $1b_2$ will also be large. Indeed the calculated D 1s orbital contribution in $1b_2$ is 54% for Pd and 38% for Ni at φ=90°, which accords with the larger destabilization of the Pd $1b_2$ level.

There is another way of analyzing this effect. The $1b_2$ orbital of MA_2D_2 is constructed in **15** from the antisymmetric D_2 combinations interacting with a bent MA_2 fragment. This interaction carries in it a substantial fraction of the M–D bond energy. Since the resulting

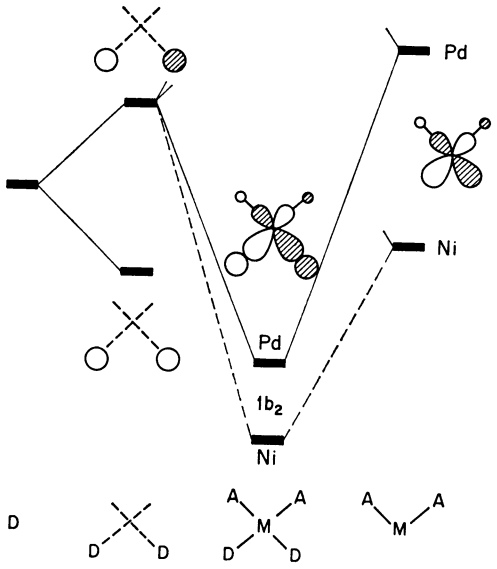

15

$1b_2$ level of $MA_2D_2^{2-}$ correlates to the b_2 of MA_2 in the D_2 elimination step, a greater energy difference between the $MA_2D_2^{2-}$ b_2 level and the MA_2^{2-} b_2 level would be associated with a greater activation energy for the reaction. The computed energy differences of the b_2 level are 2.1 eV for Pd and 1.3 eV for Ni. This is exactly what would be required to explain the different energy pattern of the Pd and Ni eliminations.

We have assigned the effect of the b_2 levels, but in fact it can be traced deeper. The b_2 level in the MA_2^{2-} fragment left behind is mainly a metal d orbital. It is higher for Pd than for Ni because the Pd and Ni d parameters are in that order. To probe this explanation we performed a numerical experiment in which D_2 was eliminated from a $MA_2D_2^{2-}$, where the M carried the Pd orbitals but with a variable 4d valence state ionization potential. The results shown on Fig. 6 clearly illustrate the dependence of the activation barrier on the metal d energy.

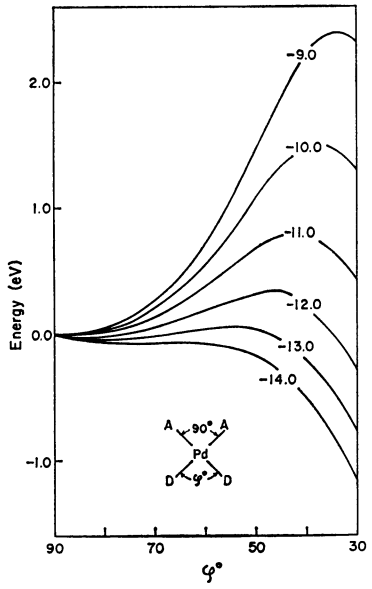

Fig. 6. The total energy of the hypothetical palladium complex $PdA_2D_2^{2-}$ as a function of the D–Pd–D angle φ. Potential curves for various choices of the "Pd" 4d ionization potential are superimposed, so that all curves are referred to an arbitrary zero of energy at $\varphi=90°$.

There is a temptation here to correlate the M–D bond strength, formed in part by this b_2 interaction, with increased activation energy to reductive elimination. Some thought about the matter, with the help of diagram **15**, shows that the relationship is not so simple. When the A_2M orbital is higher in energy than the antisymmetric combination of D orbitals, a more destabilized MA_2 b_2 would lead to a weaker M–D bond, while at the same time it would give a larger energy gap between b_2 levels of MA_2 and $MA_2D_2^{2-}$. The numerical experiment, varying M H_{ii}, that we described above, is useful in testing this supposition. Figure 7 shows how the Pd–D overlap population does not increase monotonically with higher Pd 4d energy, but peaks at the position of resonance with the D_2 antisymmetric combination. Thus, the energy gap is not always an index of the thermodynamic stability of an M–D bond, but it can be an index of the "kinetic" stability of $MA_2D_2^{2-}$ to reductive elimination.

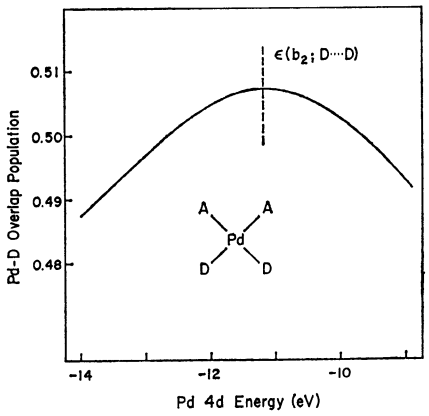

Fig. 7. Pd–D overlap population in the hypothetical palladium complex $PdA_2D_2^{2-}$ as a function of the valence state ionization potential of the Pd 4d level.

Our third conclusion: A lower positioning of the MA_2 b_2 orbital facilitates the reductive elimination of D_2. A lower MA_2 b_2 energy will be given by a lower metal d orbital energy.

While our major focus was the difference between Ni and Pd, we have also studied, albeit in abbreviated form, the Pt case. A model $PtA_2D_2^{2-}$ elimination surface gives a barrier slightly higher than in the Pd case. The Pt 5d parameters place it between Ni and Pd, but closer to Pd. The b_2 orbital is 50% on the D_2 ligands at $\varphi=90°$, a value again close to that computed for Pd. These theoretical findings are in accord with the experimental observation of difficult reductive elimination from Pt complexes.

Our next objective was to move from the model MA_2D_2 structures to more realistic models. To this end we examine reductive elimination of ethane from $Pd(PH_3)_2(CH_3)_2$, $Pd(CH_3)_4^{2-}$, and $Ni(PH_3)_2(CH_3)_2$. The essence of our orbital symmetry considerations for the hydride model system should and does carry over to those more complicated systems. Then our interest

lies in a rough theoretical estimate of the activation energies. In describing the elimination of ethane, we must consider the elongation of the Pd–C distance and the rocking motion of the methyl groups in addition to the variation of C–Pd–C angle φ and P–Pd–P angle θ. Full geometry optimization was beyond our means, so we constructed two hypothetical reation coordinates. In the first path, the P–M–P angle θ (see **16**) is fixed

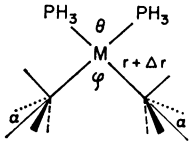

16

at 90°, while the C–Pd–C angle φ and the rocking angle α between the local three fold axis of the methyl group and the Pd–C bond extension were varied simultaneously (90—30° for φ, 0—60° for α). At the same time the Pd–C distance was stretched by Δr. The second reaction coordinate allowed θ to open from 90° to 150° while the above mentioned geometrical variations took place. We present the results for the second reaction path, the one which allows the $M(PH_3)_2$ remnant more freedom, in Fig. 8. The first reaction path differs only in destabilization of the product side.

It is clear from Fig. 8 that the calulated activation energies for ethane elimination are in the order $Pd(CH_3)_4^{2-} > Pd(PH_3)_2(CH_3)_2 > Ni(PH_3)_2(CH_3)_2$. This

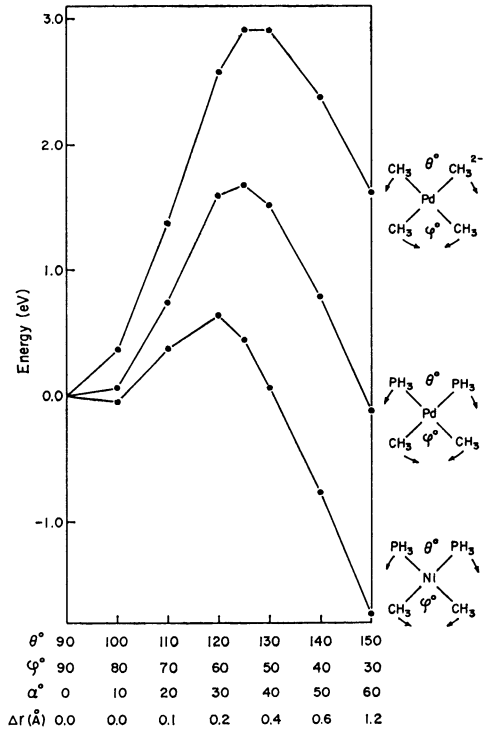

Fig. 8. Total energy changes along the hypothetical reaction path for elimination of ethane from $Pd(CH_3)_4^{2-}$, $Pd(PH_3)_2(CH_3)_2$, and $Ni(PH_3)_2(CH_3)_2$. In the reaction path the three angles and the M–C (of a leaving CH_3) distance, which are defined in **16**, are varied simultaneously. The reaction path is defined by the values or θ, φ, α, and r given at the bottom.

trend accords with our previous conclusions (2) and (3) based on the hydride model calculations. Estimated activation energies (second, more complete reaction coordinate) are around 2.9, 1.7, and 0.6 eV for $Pd(CH_3)_4^{2-}$, $Pd(PH_3)_2(CH_3)_2$, and $Ni(PH_3)_2(CH_3)_2$ respectively. These numbers are all larger than the computed activation energies of the corresponding hydride models, PdD_4^{2-}, $PdD_2A_2^{2-}$, and $PdA_2D_2^{2-}$, probably because of the bulk of the CH_3 groups and/or $Pd–CH_3$ bond weakening necessitated by the rocking motion.

We have investigated briefly the possibility of direct elimination of R_2 from a *trans*-PdR_2L_2 system through a quasi-tetrahedral transition state. The energy required to achieve such a geometry is very high, and we think this reaction mode is unlikely, at least for Pd(II) or Pt(II).

Whether a given four-coordinate complex in Scheme 1 eliminates R_2 or chooses another path, possibly ligand dissociation, depends on the relative activation energies of the various processes. Unfortunately extended Hückel calculations are not reliable for such a comparison. Nevertheless we believe that our calculations on model compounds provide a theoretical framework for understanding why the Ni complexes eliminate alkanes from the four-coordinate geometry, whereas their Pd (and Pt) analogues do different things.

Reductive Elimination from Three-coordinate Complexes.

Kinetic studies of *cis* Pd(II)[4,3] dimethyls and Au(III) trimethyls[5] indicate that elimination is preceded by a dissociative step. The resulting MLR_2 intermediate is a representative of the intriguing d^8 ML_3 class of complexes. The geometrically attractive trigonal planar structure (**7**) for these molecules turns out to be Jahn-Teller unstable in the low-spin configuration. Distortions to T or Y shaped structures (**8** or **9**) ensue. The structure of the potential energy surface is summarized in **17**.[5b] Both T and Y shaped structures should be more stable than the trigonal geometry, but which alternative is the absolute minimum cannot be easily predicted. Whichever conformation is preferred, interconversion

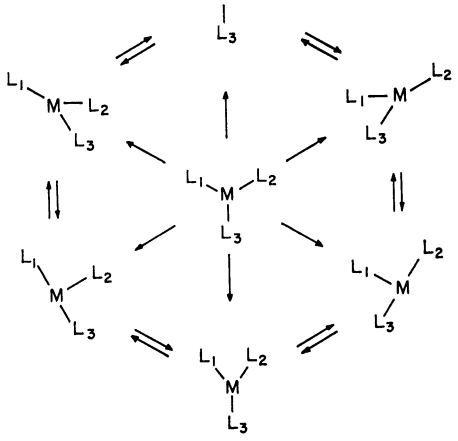

17

of isomeric C_{2v} equilibrium structures (if the ligands differ) is most unlikely to occur through the D_{3h} hill in the middle, but may proceed easily by sweeping through less symmetrical C_s waypoints along the periphery of the Jahn-Teller wheel. Direct structural evidence for deformation of d^8 ML_3 complexes is hard to come by because of the coordinative unsaturation of such 14 electron complexes. If ligand steric bulk is used to stabilize such complexes, one has to worry that the very same ligand property will also perturb the equilibrium geometry from its idealized form. One case where one can see a clear T deformation is for $Rh(PPh_3)_3^+$.[15]

What if the ligand set is substantially asymmetric, as in the $Pd(CH_3)_2(PR_3)_2$ decompositions studied by the Stille and Yamamoto groups? If phosphine dissociation occurs we are led to a three coordinate PdR_2PR_3 complex. The ligand isomerization scheme **17** simplifies to **18**. By symmetry the right-hand side of **18** is identical to the left. We will soon present a detailed analysis of this polytopal surface. For the moment let us assume that the scheme summarizes the experimental possibilities and see how it fits the available experimental data.

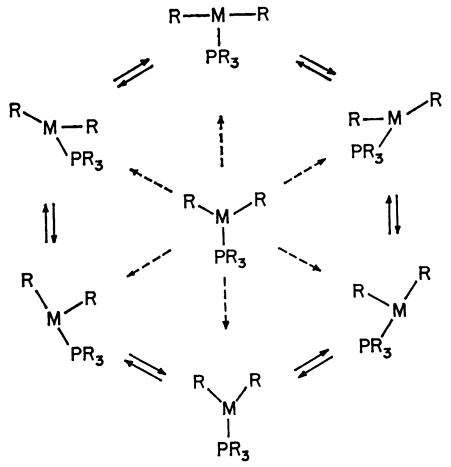

18

Least-motion departure of a phosphine from *cis* $Pd(CH_3)_2(PR_3)_2$ brings one into a T-shaped entry point in **18**, at 4 o'clock. It is easy to imagine a minor rearrangement to the Y-shapped conformer at 6 o'clock. This geometry is an obvious exit channel for elimination of R_2. Alternatively elimination could proceed directly from the T-shaped entry point.

Now consider the *trans* isomer of $Pd(CH_3)_2(PR_3)_2$. Departure of a phosphine leads one into **18** at 12 o'clock. Elimination from there is most unlikely. If the general features of the ML_3 surface were preserved one would nevertheless expect an easy transit around the Jahn-Teller wheel to 6 o'clock, the ethane exit channel. Apparently this does *not* happen. *trans* Dialkyl Pd complexes appear to be quite stable to simple reductive elimination, and instead often undergo β-elimination where that process is possible. Where reductive elimination occurs it is preceded by isomerization to the *cis* form, assisted either by polar, coordinating solvents,[4]

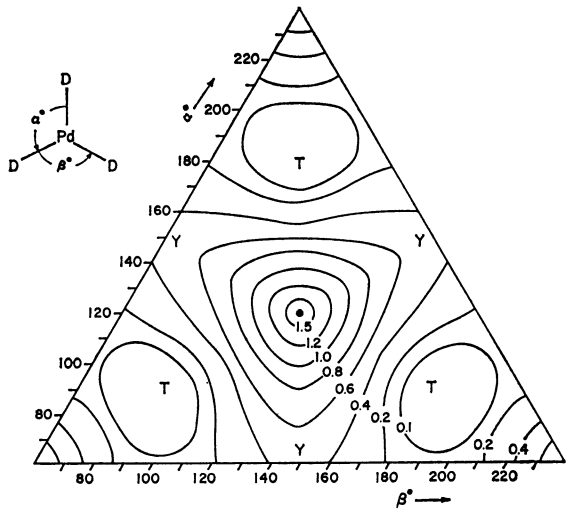

Fig. 9. Potential energy surface calculated for PdD_3^- varying the two D–Pd–D angles α and β. The energies of the contours are in electron volts relative to the T shape.

or by addition of the *cis* isomer, in an autocatalytic process.[3] Obviously the simple picture of unrestricted motion around the rim of **18** needs modification. We decided to investigate the effect of ligand electronic asymmetry on polytopal rearrangements in the three-coordinate manifold.

Again we first employ the hydride model, as we did for the four-coordinate complexes. Thus the d^8 molecules studied were PdD_3^-, $PdDA_2^-$, and $PdAD_2^-$. The characteristic features of the Jahn-Teller surface that we first delineated for $Au(CH_3)_3$ are preserved in the PdD_3^- surface (Fig. 9). A high hill of D_{3h} geometry is in the center surrounded by three descending ridges of Y-shaped geometry. Each of three equivalent T-shaped minima is in a round valley between the two ridges and has two open channels leading to reductive elimination. The activation energy for the elimination is about 0.1 eV, while the energy barrier for isomerization from one T-shape to another amounts to 0.4 eV.

The topology of the potential surface is explained by orbital diagram **19**. The half-filled e′ level immediate-

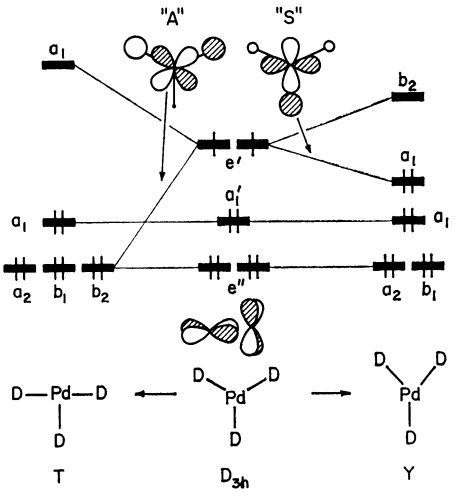

19

ly shows the Jahn-Teller instability of the D_{3h} geometry. When PdD_3^- is distorted to a T-shape, one of the e′ components, "A", is stabilized by decreasing Pd–D antibonding interaction and eventually becomes a pure Pd d orbital. On the other hand, the distortion to a Y-shape stabilizes another component, "S" of e′. But it is not by so much, because some Pd–D antibonding character still remains in the "S" component in the Y geometry. This is why the T-shape is more stable than the Y.

Potential surfaces for $PdAD_2^-$ and $PdDA_2^-$ are shown in Fig. 10. $PdAD_2^-$ will be a model for Pd-$(PR_3)(CH_3)_2$. In spite of the reduced symmetry, these surfaces maintain the basic electronic properties of the more symmetric PdD_3^-. The trigonal geometry is on a hill, and two kinds of approximate T-shapes are local minima.

Let us try to understand the relative stability of the T and Y shapes in these less symmetrical systems. We know from **19** that T is basically more stable than Y.

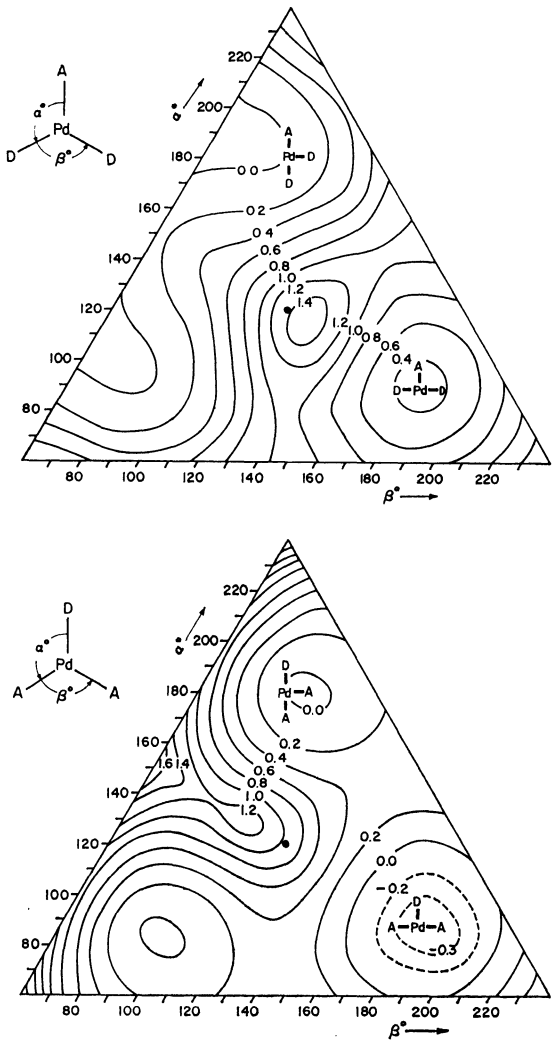

Fig. 10. Potential energy surfaces calculated for Pd-AD_2^-(top) and $PdDA_2^-$ (bottom), varying the two angles α(A–Pd–D) and β(D–Pd–D or A–Pd–A). The energies of the contours are in electron volts relative to the T shape in which one wing is occupied by D and another wing by A.

What is required is a procedure for evaluating substituent site preferences in T and Y. In the T form the occupied e′ component is "A" (see **19**) which has some ligand contribution on the wings of the T and so produces the charge distribution **20**. In the Y shape "S" is occupied, and that forces the charge imbalance shown in **21**. This is all relative to the trigonal form, where one can think of both orbitals equally occupied, by symmetry the same electron density on all ligands.

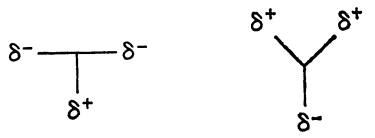

20 **21**

Now we reason that more *electronegative* substituents (poorer σ donors, better σ acceptors) will preferentially go where there is an excess of electron density.[16] The optimum substitution patterns that follow are presented in **22** and **23**. We can now summarize our qualitative

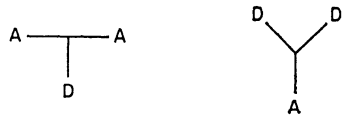

22 **23**

expectations for the relative stabilities of the asymmetric T and Y shapes, in Scheme 2. Beside some of the structures we place one or more arrows. Each indicates a stabilization, a solid arrow for the inherent greater stability of the T, a dashed arrow for fulfilling to a variable extent, the desired substitution pattern summarized in **22** or **23**. There is good qualitative agreement between Scheme 2 and the computed surfaces of Fig. 10.

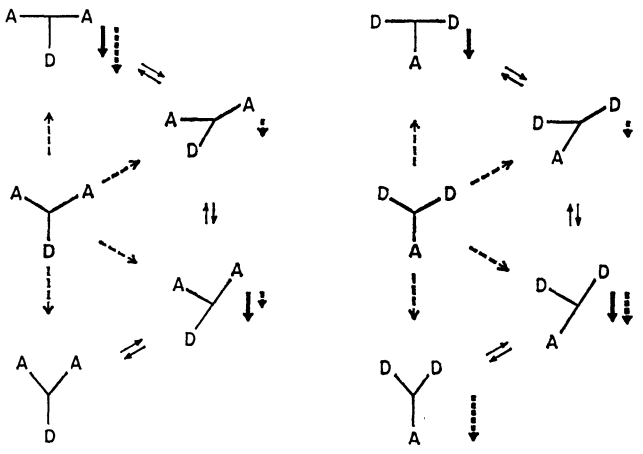

Scheme 2.

The triangular potential energy surfaces of Fig. 10 contain a great deal of interesting information. First note that reductive elimination of D_2 from **24** is just downhill in energy, while steep and high energy barriers

24 25

block the elimination of A_2 from **25**. The same trend was observed in reductive elimination from the four-coordinate system (conclusion (1))—*i.e.* a stronger σ-donor is a better leaving group. The similarity between the three- and four-coordinate systems can be traced in some detail, but the argument will not be presented here.

Another interesting consequence of the electronic asymmetry of A and D ligands to be seen from Fig. 10 is the creation of substantial energy barriers to a transit around the Jahn-Teller wheel. The activation energy for going from *trans*-$PdAD_2^-$ **26** to *cis*-$PdAD_2^-$, **27**, is

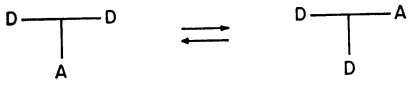

26 27

0.75 eV, and that for the reverse isomerization is 1.1 eV. Corresponding activation energies for $PdDA_2^-$ are 0.6 and 0.3 eV. Thus conclusion (4): *T-shaped* trans-$PdLR_2$, *which might be produced by liberating L from* trans-PdL_2R_2, *will encounter a substantial energy barrier to rearrangement of* cis-$PdLR_2$, *which has an open channel for reductive elimination of* R_2; *and* (5): *When the leaving groups are poor donors, A,* cis-trans *isomerization between two T-shaped geometries should be much easier than elimination of* A_2. *If R is a strong* σ *donor and L is a poor donor or an acceptor then the rearrangement from the* trans-*derived three-coordinate structure to the* cis-*derived one (motion from 12 o'clock to 4 in* **18***) will not be facile.*

These are model calculations. They were supported by detailed examination of a surface for valence tautomerism in $Pd(PH_3)(CH_3)_2$, Fig. 11. P–Pd–C angles α and C–Pd–C angle β are varied. Note the presence of three T-shaped minima, and an activation energy of 0.5 eV for the *trans*→*cis* $Pd(PH_3)(CH_3)_2$ isomerization and 0.8 eV for the reverse reaction.[23] A hypothetical reaction coordinate for ethane elimination from T- and Y-shaped conformations was also studied, modelled after the first reaction coordinate of the four-coordinate complex, discussed above. The results of such a calculation are shown in Fig. 12. As one might have guessed from the surfaces in which only angles are varied, the elimination need not proceed directly from a Y-shaped locus. Instead one can start out from a T-geometry and pay no greater price in activation energy. The computed activation energy to ethane formation along this highly simplified reaction path is 1.1 eV. The general features of this $Pd(PH_3)(CH_3)_2$ calculation are in accord with the conclusions we reached on the hydride models.

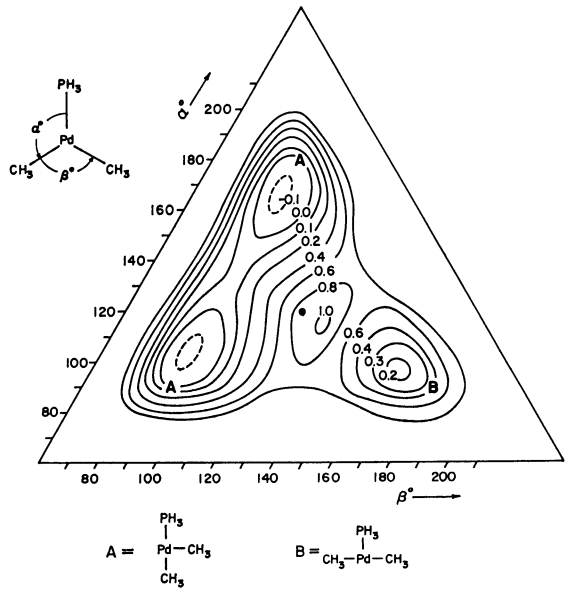

Fig. 11. Potential energy surface calculated for $Pd(PH_3)(CH_3)_2$ varying the two angles α(P–Pd–C) and β(C–Pd–C). The energies of the contours are in electron volts relative to the T shape defined by A below the triangle.

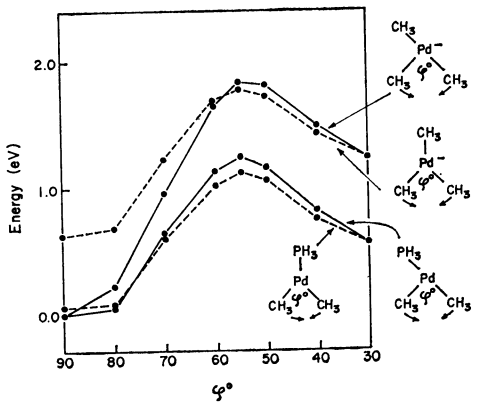

Fig. 12. Total energy changes along the hypothetical reaction path for the elimination of ethane from $Pd(CH_3)_3^-$ and $Pd(PH_3)(CH_3)_2$. The reaction path is the same one as that defined in Fig. 8, except that the angle θ is not included here. The solid lines are for the elimination reaction from the T shape while the dashed lines are for that from the Y shape.

Please return to Scheme 1, the starting point of our analysis. We have tried to elucidate but two aspects of the mechanism of reductive elimination—1. how changing the metal or the electronic properties of the ligands affects the activation energy for reductive elimination directly from the four-coordinate complex and 2. how ligand electronic asymmetry controls polytopal rearrangements, and thereby *cis-trans* isomerization and elimination, in the three-coordinate manifold. So much more remains to be understood.

We are grateful to J. Jorgensen for the drawings, to E. Stolz for the typing to the National Science Foundation for its support of this work through Research Grant CHE 7828048, and to the Exxon Education Foundation, some earlier work on $PtXY_2$ isomerizations had been carried out in our group by D. L. Thorn.

Appendix I

Our calculations are of the extended Hückel type[17] with a weighted H_{ij} approximation.[18] The Coulomb integrals and orbital exponents are listed in Table 1. The metal parameters were taken from the following sources: Exponents of Ni 3d orbitals were taken from the work of Richardson *et al.*,[19] while those of Pd 4d, 5s and 5p, and Pt 5d orbitals were from the Basch and Gray orbitals.[20] Other exponents are those given by previous work.[21] The H_{ii}'s for Pt[21] and Ni[22] are the same as those used previously. For Pd charge iterations were performed on *trans*-$Pd(CH_3)_2(PH_3)_2$ assuming a quadratic dependence of metal H_{ii}'s on charge.

TABLE 1. EXTENDED HUCKEL PARAMETERS USED IN THE CALCULATIONS

Parameters	H_{ii}/eV	Orbital exponent[a]
Ni 3d	−13.49	5.75 (0.5798) +2.30 (0.5782)
4s	−9.17	2.10
4p	−5.15	2.10
Pd 4d	−12.02	5.983 (0.5535) +2.613 (0.6701)
5s	−7.32	2.190
5p	−3.75	2.152
Pt 5d	−12.59	6.013 (0.6334) +2.696 (0.5513)
6s	−9.077	2.554
6p	−5.475	2.554
C 2s	−21.4	1.625
2p	−11.4	1.625
P 3s	−18.6	1.60
3p	−14.0	1.60
H 1s	−13.6	1.3
"D" 1s	−11.75	1.3
"A" 1s	−14.34	1.3

a) For the d functions a double zeta expansion was used. The expansion coefficients are given in parentheses.

Geometrical assumptions included the following: C–H 1.09, P–H 1.42, Ni–C 2.02, Ni–P 2.23, Pd–C 2.05, Pd–P 2.30, Ni–D(A) 1.60, Pd–D(A) 1.65, Pt–D(A) 1.75Å; PH_3 and CH_3 tetrahedral.

Appendix II

There is no unique way to define the coordinate system in the molecules under study. The "classical" choice for a four-coordinate complex, **28**, is tied to D_{4h} symmetry. It

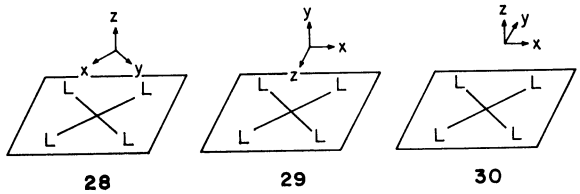

28 **29** **30**

makes the destabilized d orbital the familiar-sounding $d_{x^2-y^2}$. But the axis system of **28** is cumbersome if one wishes to study a reductive elimination that preserves C_{2v} symmetry, for the C_2 axis preserved is not one of the axes of **28**. Neither are d_{xz} and d_{yz} appropriate symmetry adapted linear combinations. **29** would be more appropriate, but it in turn loses the mnemonic connection to the classical square-planar crystal field. We choose to compromise, using **30**. This retains the z axis where the four-fold axis used to be, and allows the use of d_{xz} and d_{yz}. The price we pay is that the destabilized d orbital is d_{xy}, not $d_{x^2-y^2}$. And we have to use the non-standard character table, Table 2.

TABLE 2. C_{2v} CHARACTER TABLE USED IN THIS WORK

	E	$C_2(y)$	$\sigma(yz)$	$\sigma(xz)$
A_1	1	1	1	1
A_2	1	1	−1	−1
B_1	1	−1	1	−1
B_2	1	−1	−1	1

References

1) R. H. Grubbs, A. Miyashita, M. Liu, and P. Burk, *J. Am. Chem. Soc.*, **99**, 3863 (1977); **100**, 2418 (1978); R. H. Grubbs and A. Miyashita, *ibid.*, **100**, 1300, 7416, 7418 (1978).

2) The reductive elimination of NiR_2(dipyridyl) is accelerated by a presence of electronegative olefins, suggesting formation of five coordinated Ni complexes prior to the elimination steps; T. Yamamoto, A. Yamamoto, and S. Ikeda, *J. Am. Chem. Soc.*, **93**, 3350, 3360 (1971).

3) F. Ozawa, T. Ito, Y. Nakamura, and A. Yamamoto, *Bull. Chem. Soc. Jpn.*, see the preceding paper; F. Ozawa, T. Ito, and and A. Yamamoto, *J. Am. Chem. Soc.*, in press.

4) D. Milstein and J. K. Stille, *J. Am. Chem. Soc.*, **101**, 4981 (1979); A. Gillie and J. K. Stille, *ibid.*, **102**, 4933 (1980).

5) a) A. Tamaki, S. A. Magennis, and J. K. Kochi, *J. Am. Chem. Soc.*, **96**, 6140 (1974); A. Tamaki and J. K. Kochi, *J. Organomet. Chem.*, **40**, C81 (1972); **51**, C39 (1973). b) S. Komiya, T. A. Albright, R. Hoffmann, and J. K. Kochi, *J. Am. Chem. Soc.*, **98**, 7255 (1976); **99**, 8440 (1977).

6) a) G. M. Whitesides, J. F. Gaasch, and E. R. Stedronsky, *J. Am. Chem. Soc.*, **94**, 5258 (1972); J. X. McDermott, J. F. White, and G. M. Whitesides, *ibid.*, **98**, 6521 (1976); G. B. Young and G. M. Whitesides, *ibid.*, **100**, 5808 (1978). b) S. Komiya, A. Yamamoto, and T. Yamamoto, *Chem. Lett.*, **1978**, 1273. c) Pyrolyses of $PtL_2(R)_2$ (L=PPh_3 *etc.*, L_2=dppm, dppe, R=Ph, *p*-$CH_3C_6H_4$, and CH_3 *etc.*,) yield the reductive elimination products R–R at high temperature 150—260 °C. In this case β-hydrogen elimination cannot take place. Added phosphines enhance the reductive elimination. Five-coordinated complexes $PtL_3(R)_2$ are proposed as intermediates for the reaction; P. S. Braterman, R. J. Cross, and G. B. Young, *J. Chem. Soc., Dalton Trans.*, **1976**, 1306 and 1310; F. Glockling, T. McBride, and R. J. I. Pollock, *J. Chem. Soc., Chem. Commun.*, **1973**, 650; J. D. Ruddick and B. L. Shaw, *J. Chem. Soc., A*, **1969**, 2969.

7) M. P. Brown, R. J. Puddephatt, and C. E. Upton, *J. Organomet. Chem.*, **49**, C61 (1973); *J. Chem. Soc., Dalton Trans.*, **1974**, 2457.

8) R. J. McKinney, D. L. Thorn, R. Hoffmann, and A. Stockis, to be published.

9) R. G. Pearson, *Acc. Chem. Res.*, **4**, 152 (1971); *Pure Appl. Chem.*, **27**, 145 (1971); *Fortschr. Chem. Forsch.*, **41**, 75 (1973); "Symmetry Rules for Chemical Reactions," Wiley-Interscience, New York (1976), pp. 286, 405.

10) P. S. Braterman and R. J. Cross, *Chem. Soc. Rev.*, **2**, 271 (1973).

11) B. Åkermark and A. Ljungqvist, *J. Organomet. Chem.*, **182**, 59 (1979); B. Åkermark, H. Johansen, B. Roos, and U. Wahlgren, *J. Am. Chem. Soc.*, **101**, 5876 (1979).

12) R. B. Woodward and R. Hoffmann, *Angew. Chem.*, **81**, 797 (1969).

13) See Appendix II for a discussion of the coordinate systems.

14) The metal part of the b_2 orbital **14** (or **11**) is here

mainly d_{xy}. In our previous work on tetraalkyl gold the analogous orbital was mainly metal p_x. This is a consequence of the different metal parameters—in the Au(III) case the d orbitals were very low in energy and in metal-ligand interaction mainly metal s and p orbitals were used. In our present calculations the s and p orbitals are relatively high, and it is the metal d functions which interact most. The arguments carry through no matter which metal orbitals are involved.

15) Y. W. Yared, S. L. Miles, R. Bau, and C. A. Reed, *J. Am. Chem. Soc.*, **99**, 7076 (1977).

16) This type of argument has been successfully used by us before: R. Hoffmann, J. M. Howell, and E. L. Muetterties, *J. Am. Chem. Soc.*, **94**, 3047 (1972); A. R. Rossi and R. Hoffmann, *Inorg. Chem.*, **14**, 365 (1975); R. Hoffmann, J. M. Howell, and A. R. Rossi, *J. Am. Chem. Soc.*, **98**, 2484 (1976); R. Hoffmann, B. F. Beier, E. L. Muetterties, and A. R. Rossi, *Inorg. Chem.*, **16**, 511 (1977).

17) R. Hoffmann, *J. Chem. Phys.*, **39**, 1397 (1963); R. Hoffmann and W. N. Lipscomb, *ibid.*, **36**, 2179 (1962); **37**, 2872 (1962).

18) J. H. Ammeter, H.-B. Bürgi, J. C. Thibeault, and R. Hoffmann, *J. Am. Chem. Soc.*, **100**, 3686 (1978).

19) J. W. Richardson, R. R. Powell, and W. C. Nieuwpoort, *J. Chem. Phys.*, **38**, 796 (1963).

20) H. Basch, A. Viste, and H. B. Gray, *Theor. Chim. Acta*, **3**, 458 (1965).

21) R. H. Summerville and R. Hoffmann, *J. Am. Chem. Soc.*, **98**, 7240 (1976).

22) A charge iteration on the model porphyrin complex $Ni(NH_2)_4^{2-}$, K. Tatsumi and R. Hoffmann, to be published.

23) **Note added in proof**. A recent study, T. J. McCarthy, R. G. Nuzzo, and G. M. Whitesides, *J. Am. Chem. Soc.*, **103**, 1676 (1981) provides an excellent confirmation of our conclusions: Isotopic labeling and kinetics indicate that the two Pt-bound Et groups of a coordinatively unsaturated $Pt(PEt_3)$-Ft_2 intermediate lose hydrogen with approximately equal probability.